



Performance Analysis of the Efficiency of Cooperative Communication Systems Utilizing Radio Frequency Energy Harvesting

Tasqiatul Qulbi Kamila Huda*, I Gede Puja Astawa**(C.A.), Yoedy Moegiharto**, Mohamad Ridwan**, Budi Aswoyo**, Anang Budikarso**, Ida Anisah**, and Faridatun Nadziroh**

Abstract: The progress of 5G networks is propelled by wireless technology, specifically mobile internet and smart devices. This article provides an in-depth analysis of the fundamental elements of 5G technology, encompassing the advancement of cellular networks, simultaneous transmission capabilities, energy efficiency enhancements, and the implementation of cooperative communication. This study examines the application of simultaneous wireless information and power transfer (SWIPT) in cooperative device-to-devices (D2D) communication. Specifically, it investigates relay selection using decode-forward (DF) protocols and considers the issue of self-interference. Radio frequency based energy harvesting (RF-EH) is proposed to address power limitations in device-to-device (D2D) communication. This article describes the development of this technology and suggests a system architecture that employs time-switching relaying (TSR) techniques to enhance the power efficiency of base stations. This research aims to assess data transfer efficiency in two-way cooperative communication systems by incorporating many technologies.

Keywords: D2D Communication, DF Protocol, RF-EH with TSR, Throughput.

1 Introduction

THE development of wireless electronics propelled by mobile internet and intelligent devices, has led to the advancement of 5G. By 2020, it is anticipated that 5G networks will demonstrate benefits in terms of faster data rates, decreased delay in data transmission, broader network coverage, improved energy efficiency, less electricity consumption, and enhanced quality of experience (QoE). The essential technologies and approaches of 5G systems can be classified as follows [1–3]: the widening of cellular networks by incorporating numerous small cells and integrating peer-to-peer communication. Capabilities (such as device-to-device

(D2D) communication, enabling diverse networks); simultaneous transmitting and receiving (including Full Duplex (FD) communication); raised energy efficiency achieved by energy-aware communication and energy harvesting.

The diversity of transmission methods is advantageous for mobile base stations, particularly in elaborate scenarios involving multiple antennas on the transmitter. Nevertheless, several wireless devices are constrained in terms of their features or hardware complexity by a single antenna. Recently, a concept called cooperative communication has been introduced [4]. This concept enables mobile phones with a single antenna to share antennas in a multi-user setting, creating virtual multi-antenna transmitters. This allows transmission diversity

Iranian Journal of Electrical & Electronic Engineering, 2024.
Paper first received 21 December 2023 and accepted 23 March 2024.

* The author is student with the Department of Telecommunication Engineering, Electro Engineering Polytechnic Institute of Surabaya, Surabaya, Indonesia.
E-mail: tasqiatulqulbi@te.student.pens.ac.id.

** The authors are lecturer with the Department of Telecommunication Engineering, Electro Engineering Polytechnic Institute of Surabaya, Surabaya, Indonesia.
E-mails: puja@pens.ac.id, ymoegiharto@pens.ac.id, ridwan@pens.ac.id, budias@cepis-its.id, anang_bk@pens.ac.id, ida@pens.ac.id, faridatun@pens.ac.id.
Corresponding Author: I Gede Puja Astawa.

and uses relays to decrease power consumption in cellular networks, leading to a longer-lasting battery. A cooperative communication architecture can dramatically improve wireless capacity, data rates, and general reliability [5]. Research has also been conducted on cooperative communication and device-to-device (D2D) communication. In [6], the author indicated a collaborative transmission method for device-to-device (D2D) communication combined with cellular networks.

The researchers have also examined the integration of simultaneous wireless information and power transfer (SWIPT) systems in cooperative device-to-device (D2D) communication [7-8]. The approach of transferring electromagnetic energy has garnered attention in wireless research literature, as it involves the simultaneous transmission of information and energy using an identical waveform. The construction of a D2D node involves transmitting cellular network data using superposition coding, which allows for the simultaneous transmission of both the node's data and the data of cellular users through relays. The decode-forward (DF) protocol is a relay selection method employed in device-to-device (D2D) communication. The DF protocol operates by receiving the signal at the relay, encoding it, and re-encoding it before transmitting it to the destination. Despite its high energy consumption, DF is widely used in applications that demand superior performance [9]. While the DF protocol offers the benefit of amplifier-forward (AF) to minimize the impact of extra noise on the relay, it necessitates a greater degree of system complexity to ensure the precision of the detected signal. It indicates that the signal transmitted to the relay may be inaccurate. Due to inconsistent decoding, the DF protocol may not broadly apply to all relaying procedures. The application of full-duplex (FD) mode on relay systems is being studied. The full duplex communication system has great potential for developing 5G technology due to its advantages. One of these advantages is its ability to significantly boost spectral efficiency, up to twice as much as the half-duplex mode. Full duplex enables concurrent transmission and reception within a single time or frequency; however, it leads to significant self-interference.

During its development, battery capacity limits in D2D communications started to arise, including the time needed for recharging when the battery ran out. Energy harvesting (EH) is a viable approach in D2D communication. EH enhances efficiency and positively affects the device's lifetime [9]. Radio frequency-based energy harvesting has the potential to serve as an alternate source of energy. The RF-EH offers inherent portability, flexibility, and efficiency benefits. The RF-EH device operates within a frequency range of 0.58–3 GHz to extract energy from its surrounding environment. The RF-EH design typically comprises three main components: an information gateway, an RF energy source located on the

transmitter or base station, and additional RF environments [10]. This technology will prove highly advantageous in the wireless charging of batteries or supplying electricity to electronic devices in situations where battery replacement is challenging. Consequently, providing electricity to wireless networks in remote locations is a simple assignment.

In general, integrating the technologies mentioned earlier demonstrates a substantial advancement in wireless networks, surpassing significant barriers and paving the way for more secure applications in the future. These technologies can significantly impact several industries. There is an expectation for their rapid implementation, as they can enhance efficiency and address complicated challenges. Thus, in summary, this publication aims to assess the efficiency of the built system model. We performed a performance analysis of the throughput of a two-way cooperative communication system. We utilized the DF protocol for relay use and employed the EH-RF approach to maximize the power received from the base station.

Additionally, we implemented time-switching relaying (TSR). The application of TSR involves the nodes initially carrying out the EH procedure, followed by the subsequent transmission of signals using the remaining time. An additional noise, a self-interference (SI) placement, was introduced on the node. This will be used to compare the built-model systems later on. We use MATLAB programming language to process all the mathematical equations to signal analysis and simulation outputs from the research conducted.

The structure of this journal is as follows: The second section focuses on the design of the system models. The deduction procedure for the formula of the created model system is explained in the third section. In the fourth section, we test and analyze the experimental data. Finally, we summarise the conducted research in the fifth section.

2 System Models

The system design is illustrated in Figure 1 and Figure 2. The system model consists of two terminal nodes, S and D, connected to an entire duplex hybrid access point (HAP). The HAP transmits signals to a relay node, R, which can relay signals from one terminal node to another. The implementation of cooperative communication is employed with certain constraints involving the transmission of links from the source (S) to the destination (D) through an intermediary node (R). The node source, S, and the destination, D, both have a single antenna, but the relay, R, is equipped with two antennas, one for receiving and one for transmitting. During the transmission and reception of information, it is presumed that no direct physical connection (indirect link) is established between the nodes.

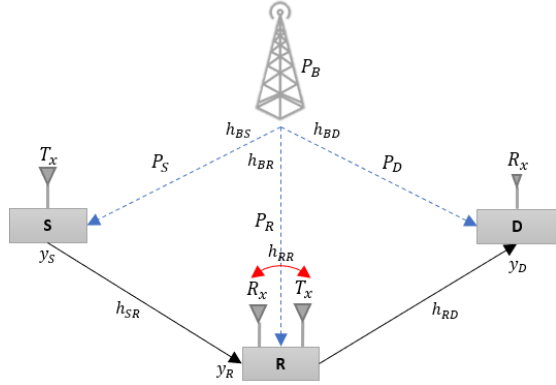


Fig. 1 First System Model, Full-Duplex with Self-Interference at R.

The EH reception assumption is derived from the base station (BS), also referred to as RF-EH. In this context, each channel coefficient is denoted by the symbol $h_{BS} = h_{BR} = h_{BD}$. These coefficients are subsequently manipulated to generate the transmitted power, P. The processing of P involves utilizing the channel gain, which is the squared magnitude of the channel coefficient, $|h_{BS}|^2, |h_{BR}|^2, |h_{BD}|^2$. The relay mechanism employed is the DF protocol, in which the relay manipulates the received signal from the source before transmitting it to the destination. The sender S transmits the information x_S through a broadcast, which is then received by the recipient R. Subsequently, the signal acquired in R, denoted as x_R , is transmitted to D as the ultimate recipient of the received information. Signal reception is observed in dimension D. The output of the decoding process at R is believed to be equal to x_R , where $x_R = x_S$, $\mathbb{E} = \|x_R^2\| = 1$: power from x_R . The chosen channel model is a Rayleigh channel, which accounts for the Non-Line of Sight (NLOS) characteristic. This implies that the signal transmission process involves traversing many trajectories. An infinite summation throughout the propagation channel determines the quality of the received signal in wireless networks. The suggested assumption for the path loss exponent is that $m = 2.7$ [11].

In the System Model 1 scenario, the presence of two antennas on R results in h_{RR} , which is referred to as self-interference. Self-interference is implemented on every node in System Model Scenario 2. Both system models assume the presence of loopback interference channels, denoted as σ_{RSI}^2 [12]. Three strategies are required to decipher the intended signal [13]. The Self Interference Cancellation (SIC) technique can be represented using Gaussian random variables that follow a normal distribution with a mean of zero and variance values of $\sigma_{SS}^2, \sigma_{RR}^2, \sigma_{DD}^2$. The residual produced by SIC can be represented as I, resulting in $I_S, I_R, I_D \sim (0, \sigma_{RSI}^2)$ [13].

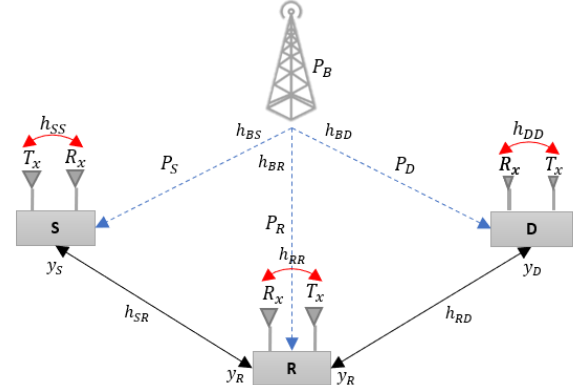


Fig. 2 Second System Model, Full-Duplex with Self-Interference at S, R, and D.

System parameters are regarded as fluctuations in measuring communication performance, specifically outage probability (OP) and throughput numbers. OP refers to the potential occurrence of an information transmission failure at its intended destination. In math, [14] represents the chance that the channel's performance will be below the given threshold or that the difference between the maximum and minimum signal-to-noise ratios will be more significant than the given threshold. The OP equation can be expressed in the following manner:

$$OP = P_R(\gamma_D < \gamma_{th}) \quad (1)$$

Performance evaluation with throughput parameters can be written with the following equation:

$$\tau = (1 - OP)R/2 \quad (2)$$

Where R is the fixed source transmission rate.

3 Performance Analysis

3.1 Energy Harvesting Process

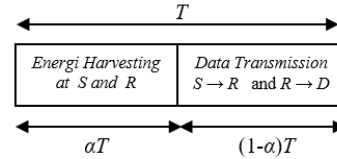


Fig. 3 EH-RF Diagram

The channel coefficients between the base stations (BS) and the locations S, R, and D are denoted as h_{BS}, h_{BR} , and h_{BD} , respectively. Additionally, the channels between S and R and R and D are denoted as h_{SR} and h_{RD} . All these channels are presumed to possess a weakened Rayleigh block, with a constant channel gain value for each signal delivery block and a random variation for each shift in the delivery block. In this system model, the duration of one

signal transmission block is denoted as T. As the energy harvesting (EH) process is implemented using the time-switching protocol, each signal transfer block is separated into two time slots.

During the initial time slot of αT (where $0 \leq \alpha \leq 1$ and α represents a time-sharing factor), S and R receive a radio frequency (RF) signal from the base station (BS) and carry out an energy download procedure. This process involves converting an alternating current (AC) RF signal into a direct current (DC) signal to exchange it for charging. Subsequently, S utilizes all the acquired power from the download procedure to transmit a signal to R during the second time slot $(1 - \alpha)T$. Additionally, during this second slot, R concurrently transfers the signal received from S to D. The temporal allocation for the energy transfer and information transmission procedures is illustrated in Figure 3 [15].

The initial process in the system involves the transmission of energy. Figure 3 displays the TSR protocol settings of the EH and information transmission processes. During this procedure, the initial block time, αT takes place. The reception process of RF-EH on each node can be expressed as follows:

$$E_S = \eta_S |h_{BS}|^2 d_{BS}^{-m} P_B \alpha T \quad (3)$$

$$E_R = \eta_R |h_{BR}|^2 d_{BR}^{-m} P_B \alpha T \quad (4)$$

$$E_D = \eta_D |h_{BD}|^2 d_{BD}^{-m} P_B \alpha T \quad (5)$$

Equation (3-5) represents the gain channel utilized by each channel throughout the RF-EH process. Therefore, while determining the distance between nodes and the base station, the path-loss exponent [26] must be considered. The power of each node is determined by dividing the output of the RF-EH process by the succeeding block time, $(1 - \alpha)T$. Below are the power equations for S, R, and D:

$$P_S = \frac{E_S}{(1-\alpha)T} = P_B \eta_S (|h_{BS}|^2 d_{BS}^{-m}) \frac{\alpha}{(1-\alpha)} \quad (6)$$

$$P_R = \frac{E_R}{(1-\alpha)T} = P_B \eta_R (|h_{BR}|^2 d_{BR}^{-m}) \frac{\alpha}{(1-\alpha)} \quad (7)$$

$$P_D = \frac{E_D}{(1-\alpha)T} = P_B \eta_S (|h_{BD}|^2 d_{BD}^{-m}) \frac{\alpha}{(1-\alpha)} \quad (8)$$

As the outcome of the RF-EH process influences the anchor power, the traversed channel remains the channel connecting the base station to the corresponding nodes.

The system model presented includes a relay, source, and destination denoted as R, S, and D, respectively. These components are depicted in Figure 1 and Figure 2. It is inferred that there is no direct contact between S and D due to the presence of impediment items that attenuate the signal received by D from S. R initially receives the signal and subsequently transmits it to D using the relay protocol decode and forward (DF).

3.2 FD with Self-Interference at R

In the initial scenario of the S and D system, a single antenna is used for transmitting and receiving signals, and it operates in a half-duplex mode. On R, a single receiving antenna and a single transmitting antenna operate independently and in full duplex mode, as shown in Figure 1a. To achieve full-duplex communication, R transmits a signal to D or S within the same time slot as the previously received signal. Furthermore, the signal processing time in R is seen as equivalent to a signal period's duration. In the R programming language, interference cancellation is used to mitigate the reverse interference caused by the transmitter and reception antennas. Due to imperfect removal, there is residual loop interference known as I_{RR} , which is modeled as a Gaussian random variable with an average value of zero and a variance of σ_{RSI}^2 [6] [16].

The process of signal reception is studied in research and development. The signal sent from S and the presence of SI, which acts as additive white Gaussian noise (AWGN) in R, change how the signal is received in R. During the reception operation, the signal is subject to interference from R and noise. However, in this process, the signal at x_R is decoded. Below is the equation representing the signal received in the R and D:

$$y_R(t) = \sqrt{P_S} h_{SR} \sqrt{d_{SR}^{-m}} x_S(t) + h_{RR} x_R(t) + n_R(t) \quad (9)$$

$$y_D(t) = \sqrt{P_R} h_{DR} \sqrt{d_{DR}^{-m}} \hat{x}_R(t) + n_D \quad (10)$$

In the scenario where the DF protocol is implemented, the signal broadcast from the source and relay is denoted as x_S and x_R , respectively, with $x_S = x_R$. The variables n_R and n_D represent additive white Gaussian noise (AWGN) with zero mean and variances σ_R^2 and σ_D^2 , respectively; $n_R \sim \mathcal{CN}(0, \sigma_R^2)$ and $n_D \sim \mathcal{CN}(0, \sigma_D^2)$ [27].

As elucidated, h_{RR} denotes the representation of the signal intensity (SI) in R. It is characterized by considerably higher values than the noise introduced from S. This discrepancy arises due to the proximity between the transmitter antenna and the receiver in R. Subsequently, the outcome is acquired through the residual loopback interface channel using I_{RR} . The signal received in R after successive interference cancellation (SIC) can be expressed as:

$$y_R(t) = \sqrt{P_S} h_{SR} \sqrt{d_{SR}^{-m}} x_S(t) + I_{RR} + n_R(t) \quad (11)$$

The SNR received in D can be obtained by using the substitutional equation (3–11) as follows:

$$\gamma_D = \frac{P_R H_{RD}}{\sigma_D^2}, = \frac{P_R |h_{RD}|^2 d_{RD}^{-m}}{\sigma_D^2}$$

$$\gamma_D = \frac{P_B \eta_R (|h_{BR}|^2 d_{BR}^{-m}) \frac{\alpha}{(1-\alpha)} H_{RD}}{\sigma_D^2}$$

$$\gamma_D = \frac{\alpha}{(1-\alpha)} \frac{P_B \eta_R H_{BR} H_{RD}}{\sigma_D^2} \quad (12)$$

The term, $H_{RD} = \frac{|h_{RD}|^2}{d_{RD}^m}$ and σ_D^2 represents the additive white Gaussian noise with zero mean. The average throughput of a system can be determined by calculating the outage probability (OP) using a given transmission rate measured in bits per second per hertz (bps/Hz). The throughput in a full-duplex TSR scenario can be expressed as:

$$\tau = \frac{(1 - \text{prob})R}{2}$$

$$= \frac{(1 - (\text{prob}(\gamma_D < \gamma_{th})))R}{2}$$

$$= \frac{\left(1 - \left(\text{prob}\left(|h_{RD}|^2 < \frac{\sigma_D^2 \gamma_{th}}{2P_B \eta_R (|h_{BR}|^2 d_{BR}^{-m}) A d_{RD}^m}\right)\right)\right)R}{2} \quad (13)$$

The variables, $A = \frac{\alpha}{(1-\alpha)}$, and outage probability (OP) can be defined as follows:

$$OP = \text{prob}(\gamma_D < \gamma_{th})$$

$$= \text{prob}\left(\frac{2P_B \eta_R (|h_{BR}|^2 d_{BR}^{-m}) \frac{\alpha}{(1-\alpha)} H_{RD}}{\sigma_D^2} < \gamma_{th}\right)$$

$$= \text{prob}\left(\frac{2P_B \eta_R (|h_{BR}|^2 d_{BR}^{-m}) \frac{\alpha}{(1-\alpha)}}{|h_{RD}|^2 d_{RD}^m} < \gamma_{th}\right)$$

$$= \text{prob}\left(|h_{RD}|^2 < \frac{\sigma_D^2 \gamma_{th}}{2P_B \eta_R (|h_{BR}|^2 d_{BR}^{-m}) A d_{RD}^m}\right) \quad (14)$$

The equation is defined as $\gamma_{th} = \frac{R}{2(1-\alpha)}$.

3.3 FD with Self-Interference at S, R, and D

The primary distinction between the 1st and 2nd systematic models is the inclusion of SIC functions in every node of the 2nd system model. In the second situation, denoted as S, R, and D, a single reception antenna and a single sender antenna operate in full duplex mode. In the programming languages R and D, an interference cancellation procedure is utilized to mitigate the reverse interference caused by the transmitter and receiver antennas. Due to the imperfect performance of the interference removal process, there remains a residual loop interference in D. This interference is represented as

a Gauss random variable with an average value of zero and a convexity of σ_{RSI}^2 .

Another distinction lies in R's simultaneous transmission and reception process, where the received signal originates from both S and D, thereby influencing it. The signal received in D is exclusively influenced by the signal originating from R and the interference caused by SIC. The signals received in research and development (R and D) can be expressed as follows:

$$y_R(t) = \sqrt{P_S} h_{SR} \sqrt{d_{SR}^{-m}} x_S(t) + I_{RR} + n_R(t) \quad (15)$$

$$y_D(t) = \sqrt{P_R} h_{DR} \sqrt{d_{DR}^{-m}} \hat{x}_R(t) + h_{DD} x_D(t) + n_D \quad (16)$$

where, $\hat{x}_R(t) = x_S(t-1)$

The variables n_R and n_D represent the additive white Gaussian noise (AWGN). The influence arises from the generation of residual loopback interference channels. RSI, which stands for Relative Strength Index, is sometimes referred to as the Gaussian complex with a variance of σ_{RSI}^2 . The equation (15–16) can be restated as:

$$y_R = \sqrt{P_S} \frac{h_{SR}}{\sqrt{d_{SR}^m}} x_S + \sqrt{P_D} \frac{h_{RD}}{\sqrt{d_{RD}^m}} x_D + \sqrt{P_R} I_R + n_R \quad (17)$$

$$y_D = \sqrt{P_R} \frac{h_{RD}}{\sqrt{d_{RD}^m}} x_R + \sqrt{P_D} I_D + n_D \quad (18)$$

The signal-to-noise ratio (SNR) value in D can be found using the equation that considers the signal-receiving process.

$$\gamma_D = \frac{2P_B \eta_R (|h_{BR}|^2 d_{BR}^{-m}) \frac{\alpha}{(1-\alpha)} H_{RD}}{(2P_B \eta_S (|h_{BD}|^2 d_{BD}^{-m}) \frac{\alpha}{(1-\alpha)}) \sigma_{DD}^2 + \sigma_D^2}$$

$$\gamma_D = \frac{P_R H_{RD}}{P_D I_D + \sigma_D^2} \quad (19)$$

The subsequent evaluation of the system's performance is attributed to the high value of the throughput and output. The throughput on system model 2 can be expressed.

$$\tau = \frac{(1 - \text{prob})R}{2}$$

$$= \frac{(1 - (\text{prob}(\gamma_D < \gamma_{th})))R}{2}$$

$$= \frac{\left(1 - \left(\text{prob}\left(|h_{RD}|^2 < \frac{\sigma_D^2 \gamma_{th}}{2P_B \eta_S (|h_{BD}|^2 d_{BD}^{-m}) A} \frac{\sigma_{DD}^2 + \sigma_D^2}{2P_B \eta_R (|h_{BR}|^2 d_{BR}^{-m}) A d_{RD}^m}\right)\right)\right)R}{2} \quad (20)$$

Outage probability (OP), respectively.

$$\begin{aligned}
OP &= \text{prob} (\gamma_D < \gamma_{th}) \\
&= \text{prob} \left(\frac{2P_B \eta_R (|h_{BR}|^2 d_{BR}^{-m})^{\frac{\alpha}{1-\alpha}} H_{RD}}{(2P_B \eta_S (|h_{BD}|^2 d_{BD}^{-m})^{\frac{\alpha}{1-\alpha}}) \sigma_{DD}^2 + \sigma_B^2} < \right. \\
&\quad \left. \gamma_{th} \right) \\
&= \text{prob} \left(2P_B \eta_R (|h_{BR}|^2 d_{BR}^{-m})^{\frac{\alpha}{1-\alpha}} |h_{RD}|^2 d_{RD}^m < \right. \\
&\quad \left. (2P_B \eta_S (|h_{BD}|^2 d_{BD}^{-m})^{\frac{\alpha}{1-\alpha}}) \sigma_{DD}^2 + \sigma_B^2 \gamma_{th} \right) \\
&= \text{prob} \left(|h_{RD}|^2 < \frac{(2P_B \eta_S (|h_{BD}|^2 d_{BD}^{-m})^{\frac{\alpha}{1-\alpha}}) \sigma_{DD}^2 + \sigma_B^2 \gamma_{th}}{2P_B \eta_R (|h_{BR}|^2 d_{BR}^{-m})^{\frac{\alpha}{1-\alpha}} d_{RD}^m} \right) \quad (21)
\end{aligned}$$

The substitutional equation solutions (3–21) represent the outcomes of a full-duplex TSR scenario, which may be confirmed by examining the simulation results presented in Section 4.

4 Result and Discussion

4.1 Parameters

Analyses are conducted to determine the system models' optimal performance to identify the perfect model for future system design. An analysis of the system testing result is conducted using a graph located on side D. The following parameters are used: Variation in the conversion efficiency coefficient Efficiency, or η_R : The value η_R is utilized during the process of energy harvesting (EH). The value of η_R directly impacts the energy or power received by each node, affecting the system performance and the D's signal-to-noise ratio (SNR).

The value of R plays a crucial role in this relationship. The value of η_R provided during the system test falls within the range of $0 < \eta < 1$, explicitly starting at 0.5 and incrementing by 0.1 up to 0.9. Second, the time block coefficient represents the time block's division by the time factor of switching, which is responsible for the EH process, transmission, and reception of information. During the initial sub-time of an EH (Energy Harvesting) process, energy is transferred from the base station to S, R, and D for a duration of αT . The information transmission procedure to R takes a second-time length of $(1 - \alpha)T$, followed by the subsequent transfer of information from R to D, which lasts for a duration of $(1 - \alpha)$.

Table 1 Simulation Parameters

Symbol	Numeric	Dec
N	10^5 binary bit	Number of binary bits
m	2.7	Pathloss component
R	2	Transmitted rate
N_0	-70 dBm	Noise power
I_D, I_R	-30 dBm	Self-interference
P_{BS}	20-26 dBW	Base station power

4.2 Performance analysis with η_R variance

The test parameters include the fluctuation of the efficiency of the EH factor, which will be used to obtain results for the previously designed best model system. The detected signal represents the amount of data transmitted by the receiver.

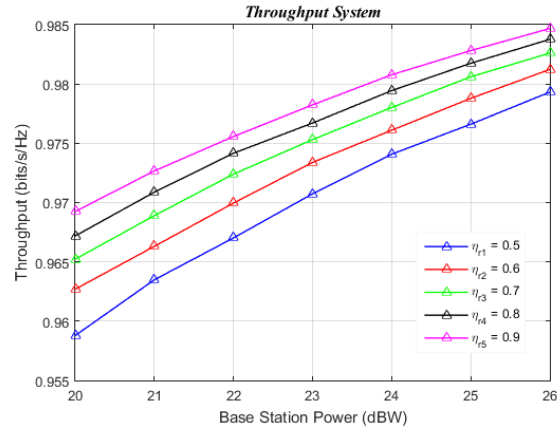


Fig. 4 Throughput Graph with η_R Variance on the First System Model

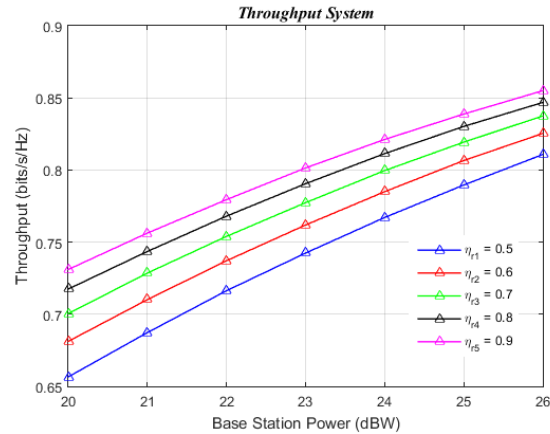


Fig. 5 Throughput Graph with η_R Variance on the Second System Model

The resulting throughput value. In more detail, when the efficiency factor was EH 0.5 with a transmit power of 26 dBW, the throughput achieved was 0.9793 bps/Hz for the first model system and 0.8108 bps/Hz for the second model system. Furthermore, with the same power and an EH efficiency factor variance of 0.9, the first model system produced a throughput of 0.9847 bps/Hz and 0.8550 bps/Hz for the second model system.

Table 2 SNR Result with η_R Variance

$P_{BS} = 26 \text{ dBW}$		
α	1 st model	2 nd model
0.4	52.05 dBW	35.32 dBW
0.5	52.84 dBW	36.11 dBW
0.6	53.51 dBW	36.78 dBW
0.7	54.09 dBW	37.36 dBW
0.8	54.60 dBW	47.87 dBW

The table displays the maximum signal-to-noise ratio (SNR) achieved on the initial system model using the highest efficiency factor (EH) value of 0.9 and the maximum base station (BS) power of 26 dBW. The value is impacted by various aspects, including diverse designs that yield distinct SNR and throughput values.

4.3 Performance analysis with Alpha variance

Investigations are conducted on two systems specifically designed to modify the value of the time-sharing coefficient, also known as α . The function to calculate the throughput will be determined based on the received SNR value in D.

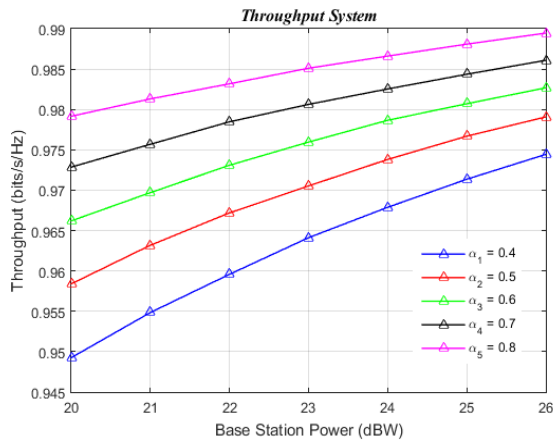


Fig. 6 Throughput Graph with Alpha Variance on the First System Model

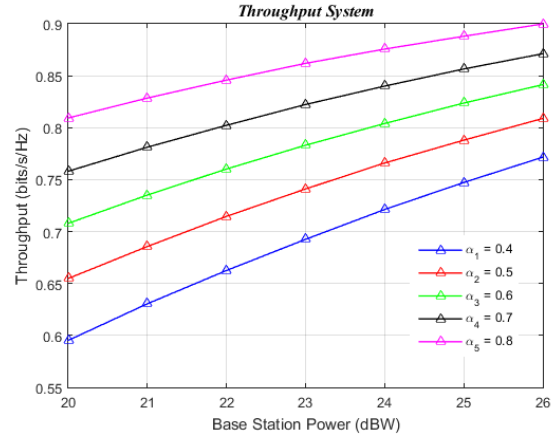


Fig. 7 Throughput Graph with Alpha Variance on the Second System Model

In this case, increasing the alpha value and the power of the BS results in a higher throughput value for each model system. In the first model system ($P_{BS} = 26 \text{ dBW}$), the maximum value is achieved at alpha 0.8 with an output of 0.9895 bps/Hz, whereas at alpha 0.4, the output value is 0.9744 bps/Hz. In the second model system ($P_{BS} = 26 \text{ dBW}$), specifically at Alpha 0.8, the throughput is measured at 0.8999 bps/Hz. The outputs in version 0.4 of the emulator are 0.7716 bps/Hz.

Table 3 SNR Result with Alpha Variance

$P_{BS} = 26 \text{ dBW}$		
α	1 st model	2 nd model
0.4	48.55 dBW	35.41 dBW
0.5	50.31 dBW	37.17 dBW
0.6	52.08 dBW	38.93 dBW
0.7	53.99 dBW	40.85 dBW
0.8	56.33 dBW	43.19 dBW

Table 3 indicates that the first model system outperforms the second model system. One of the influences is self-interference with the node. In the second model system, the entire node is intentionally constructed with self-interference, introducing more noise.

Numerous crucial elements must be taken into account to optimize system performance. An essential element involves evaluating the findings from prior research as documented in relevant academic journals. Prior research findings might be a foundation for making informed judgments while creating and optimizing systems.

Furthermore, the value assigned to the test parameter is a crucial factor in guaranteeing the highest level of performance. The analysis results indicate that the EH efficiency factor and the time block factor value achieve their optimal level as they approach or go below 1. Hence,

employing a test parameter value close to this limit can prove to be a highly successful approach for attaining optimal system performance.

Within the framework of model systems, the findings indicated that the initial model, which was constructed with complete duplex capability and one self-interference in R, exhibited the most superior performance. By employing this configuration, the system prevented interference with the reception of signals in D, resulting in superior performance values compared to the second system model.

In contrast, the second model system introduces self-interference to each node, resulting in increased noise throughout the signal-receiving process in D. This issue arises because of the combined impact of antennas and devices, leading to suboptimal performance compared to the initial model system. Hence, when developing a system, it is crucial to consider the influence of the configuration and test settings on the total performance.

5 Conclusion

This article examines the application of RF-EH through the implementation of the TSR protocol and the utilization of the DF protocol on relays for two-way cooperative communication model systems. A proposed SI delivery strategy introduces additional noise on the D2D device. Both model systems were tested using the EH efficiency factor and the time switching factor. The test findings indicate that the parameters and the high-power base station impact the throughput value. In system model 1, the α parameter, which represents the TSR factor, has a notable influence on the efficiency of the EH process. As the value of α increases, the throughput also increases, decreasing the risk of an interruption. This is demonstrated by the outcome presented in the initial model system. At $\alpha = 0.4$, the throughput achieved is 0.9744 bps/Hz, whereas at $\alpha = 0.9$, the value acquired is 0.9895 bps/Hz. A similar phenomenon occurs with the parameter η_R , whereby the escalating efficiency factor EH will inevitably result in a substantial throughput value. In the second model system, when η_R is 0.9, the result is 0.8550 bps/Hz, and when η_R is 0.5, the value is 0.8108 bps/Hz. Therefore, the study reveals that high throughput values are achieved when the values of η_R and α are close to or less than 1. High throughput values are directly impacted by high base station (BS) power levels, as evidenced by the graphical representation showing an increasing trend corresponding to the magnitude of the BS power. For instance, the highest value is achieved in both model systems when the base station power is set at 26 dBW. Moreover, models 1 and 2 systems are evaluated, specifically focusing on the achieved throughput and SNR values. In system model 2, when each node is provided with SI, there is a reduction in both throughput and SNR. This demonstrates that the SI exerts an impact

on the information that is to be received. System model 2, incorporating the SI in every node, has a signal-to-noise ratio (SNR) of 43.19 dBW. This number is lower than the system Model 1, where the SI is only present at one point, precisely at R, resulting in an SNR of 56.33 dBW with an alpha variance of 0.9. Based on the journal, it can be inferred that the model system with the lowest SI achieves the highest performance.

References

- [1] P. Demestichas, A. Georgakopoulos, D. Karvounas, K. Tsagkaris, V. Stavroulaki, J. Lu, C. Xiong, and J. Yao, "5G on the horizon: Key challenges for the radio-access network," *IEEE Veh. Technol. Mag.*, vol. 8, no. 3, pp. 47–53, Sept. 2013.
- [2] A. Zakrzewska, S. Ruepp, and M. Berger, "Towards converged 5G mobile networks - Challenges and current trends," in *Proc. ITU Kaleidoscope Academic Conf.*, pp. 39–45, Jun. 2014.
- [3] S. Talwar, D. Choudhury, K. Dimou, E. Aryafar, B. Bangerter, and K. Stewart, "Enabling technologies and architectures for 5G wireless," in *Proc. IEEE MTT-S Int. Microwave Symp. (IMS)*, pp. 1–4, Jun. 2014.
- [4] T. Wu and H. C. Yang, "RF energy harvesting with cooperative beam selection for wireless sensors," *IEEE Wirel. Commun. Lett.*, vol. 3, no. 6, pp. 585–588, 2014.
- [5] N. T. Malik, A. T. Abdulsadda, and A. J. Al Yasiri, "Relaying protocols for wireless energy harvesting and information processing," *Int. J. Eng. Adv. Technol.*, vol. 9, no. 1, pp. 1740–1746, 2019.
- [6] S. Shalmashi and S. Ben Slimane, "Cooperative device-to-device communications in the downlink of cellular networks," in *Wireless Communications and Networking Conference (WCNC), 2014 IEEE*. IEEE, 2014, pp. 2265–2270.
- [7] M. Seif, A. El-Keyi, K. G. Seddik and M. Nafie, "Cooperative D2D communication in downlink cellular networks with energy harvesting capability," 2017 13th International Wireless Communications and Mobile Computing Conference (IWCMC), Valencia, 2017, pp. 183–189.
- [8] J. Huang, J. Cui, C. -C. Xing and H. Gharavi, "Energy-Efficient SWIPT-Empowered D2D Mode Selection," in *IEEE Transactions on Vehicular Technology*, vol. 69, no. 4, pp. 3903–3915, April 2020.
- [9] A. C. C. Chun, H. Ramiah, and S. Mekhilef, "Wide Power Dynamic Range CMOS RF-DC Rectifier for RF Energy Harvesting System: A Review," *IEEE Access*, vol. 10, pp. 23948–23963, 2022.

- [10] O. L. A. Lopez, B. Clerckx, and M. Latva-Aho, "Dynamic RF Combining for Multi-Antenna Ambient Energy Harvesting," *IEEE Wirel. Commun. Lett.*, vol. 11, no. 3, pp. 493–497, 2022.
- [11] L. Mubarakah, "Pengukuran Dan Perhitungan Path Loss Eksponen Untuk Cluster Residences, Central Business Distric (CBD), Dan Perkantoran Di Daerah Urban," EEPIS Final Project, 2011.
- [12] B. C. Nguyen and X. N. Tran, "Performance analysis of full-duplex amplify-and-forward relay system with hardware impairments and imperfect self-interference cancellation," *Wirel. Commun. Mob. Comput.*, vol. 2019.
- [13] B. C. Nguyen, X. N. Tran, T. T. H. Nguyen, and D. T. Tran, "On Performance of Full-Duplex Decode-and-Forward Relay Systems with an Optimal Power Setting under the Impact of Hardware Impairments," *Wirel. Commun. Mob. Comput.*, vol. 2020.
- [14] V. D. Nguyen, S. Dinh-Van, and O. S. Shin, "Opportunistic relaying with wireless energy harvesting in a cognitive radio system," *2015 IEEE Wirel. Commun. Netw. Conf. WCNC 2015*, no. Wcnc, pp. 87–92, 2015.
- [15] X. Zhou, R. Zhang, and C. K. Ho, "Wireless information and power transfer: architecture design and rate-energy tradeoff," 2012. Available: <http://arxiv.org/abs/1205.0618>.
- [16] Yazlin, Alvis; dkk. "Performansi Sistem Komunikasi Kooperatif Menggunakan Teknik Amplify and Forward (Af) Dengan Modulasi Quadrature Phase Shift Keying (Qpsk)." *Neliti, Jurnal Mahasiswa Teknik Elektro Universitas Brawijaya*, 1–9, 2014.



Tasqiatul Qulbi Kamila Huda was born in 2000 in Yogyakarta, Indonesia. She received the Diploma Engineering in Telecommunication Engineering from State Polytechnic of Malang in 2023. In 2024, she received her B.Sc. degree from Politeknik Elektronika Negeri Surabaya, Indonesia. Her research interests include the implementation of 5G technology and data communication.



I Gede Puja Astawa was born in 1967 in Buleleng, Bali Island, Indonesia. He received his B.Sc. and M.Sc. degrees from Institute of Technology Sepuluh Nopember in Surabaya in 1993 and 2016, respectively all in Electrical Engineering. In 2012, He received his Ph.D. (Doctor of Engineering) degree from Nara Institute of Science and Technology in Japan. He is currently

working in the Department of Electrical Engineering at Politeknik Elektronika Negeri Surabaya (PENS) in Surabaya, Indonesia since 1994 until now. His field of interest includes Wireless Communication and Signal Processing.



Yoedy Moegiharto, He received his B.Sc. and M.Sc. degrees from Institute of Technology Sepuluh Nopember in Surabaya in 1984 and 2000, respectively all in Electrical Engineering. He is working in the Department of Electrical Engineering at Politeknik Elektronika Negeri Surabaya (PENS) in Surabaya, Indonesia since 1990 until 2023. His field of interest

includes Telecommunication and Electronic Circuits



Mohamad Ridwan, He received his B.Sc. and M.Sc. degrees from Institute of Technology Sepuluh Nopember in Surabaya in 2013 and 2018, respectively all in Electrical Engineering. He is working in the Department of Electrical Engineering at Politeknik Elektronika Negeri Surabaya (PENS) in Surabaya, Indonesia since 2019 until now. His field of interest

includes Network Computer, Microcontroller, Electronic Circuits.



Budi Aswoyo, He received his B.Sc. and M.Sc. degrees from Institute of Technology Sepuluh Nopember in Surabaya in 1988 respectively all in Electrical Engineering. He is currently in the Department of Electrical Engineering at Politeknik Elektronika Negeri Surabaya (PENS) in Surabaya, Indonesia since 1989 until now. His field of interest includes

Telecommunication, Antenna Design and Propagation Wave.



Anang Budikarso, He received her B.Sc. and M.Sc. degrees from Institute of Technology Sepuluh Nopember in Surabaya in 1994 and 2004, respectively all in Electrical Engineering. He is currently in the Department of Electrical Engineering at Politeknik Elektronika Negeri Surabaya (PENS) in Surabaya, Indonesia since 1988 until now His field of interest includes Telecommunication, Logic Design,

Microcontroller and Electronic Circuits.



Faridatun Nadziroh, She received his B.Sc. and M.Sc. degrees from Politeknik Elektronika Negeri Surabaya in Surabaya and Technology Sepuluh Nopember in Surabaya in 2013 and 2015, respectively all in Electrical Engineering. She is currently in the Department of Electrical Engineering at Politeknik Elektronika Negeri Surabaya (PENS) in Surabaya,

Indonesia since 2022 until now. Her field of interest includes Multimedia Telecommunication and Electronic Circuits.



Ida Anisah, She received her B.Sc. and M.Sc. degrees from Politeknik Elektronika Negeri Surabaya in Surabaya and Technology Sepuluh Nopember in Surabaya in 2012 and 2014, respectively all in Electrical Engineering. She is currently in the Department of Electrical Engineering at Politeknik Elektronika Negeri Surabaya (PENS) in Surabaya, Indonesia since 2015 until now. Her

field of interest includes Multimedia Telecommunication and Telecommunication of Network Security.